Proc. of the 8th International Symposium on Geotechnical Safety and Risk (ISGSR)
Edited by Jinsong Huang, D.V. Griffiths, Shui-Hua Jiang, Anna Giacomini and Richard Kelly
 Published by Research Publishing, Singapore.
doi: 10.3850/978-981-18-5182-7_18-005-cd

Reliability Approaches to Overcome Load-Resistance Duality in Embedded Wall Design

Álvaro J. Mattos[1]andEdwin F. García[1]

[1]Environmental School, Faculty of Engineering, Univ. of Antioquia, Medellín 050010, Colombia.
E-mail: alvaro.mattos@udea.edu.co; edwin.garcia@udea.edu.co

Abstract: In this paper, the limit-state design approaches of the AASHTO LRFD BDS and EN 1997-1:2004 codes for the design of an embedded wall are characterized. The rotational, hydraulic, and system failures of the wall are analyzed by two reliability approaches:MCS-based probabilistic and GSS-based full probabilistic design approaches. The potentialities and limitations of the reliability approaches at small- and high-reliability levels ($1 \leq \beta \leq 6$)are detailed. Three types of uncertainties and uncertainty propagation that affect the reliability approaches are discussed. The reliability levels of the limit-state design approaches are evaluated considering the highest variability of cohesionless soils reported in the literature. The GSS results show that the embedment depth of the wall exhibits a dual behavior (stabilizing-destabilizing) on the system failure at high reliability levels.

Keywords: Embedded wall;load-resistance duality;standards and codes;limit-state design; uncertainty modeling.

1 Introduction

Partial factor-based limit-state design approaches used by geotechnical codes of practice and standards have been successfully applied to foundation design but have been less satisfactory when applied to earth-retaining walls (Christian and Baecher 2011). In the design of earth-retaining walls, one of the significant challenges is that the load and resistance generally originate from the same source (e.g., unit weight of soil) and are correlated with each other. This has led practitioners, designers, and academics to ask whether passive pressure should be regarded as a load or a resistance. The answer to this question has a significant bearing and may result in different designs because the partial factors are different for resistances and loads (Wang et al. 2016). The difficulty of handling correlated loads and resistances can be overcome using comprehensive probabilistic design approaches, as does the ISO 2394:2015 code. However, the process of overcoming load-resistance duality is sensitive to several reliability-based design (RBD) considerations (Low and Bathurst 2021; Mattos 2022).

This study analyzes the relationships and limitations of full-probabilistic design approaches and partial factor-based limit-state design approaches for an embedded wall designed to the EN 1997-1:2004 and AASHTO LRFD BDS codes. The design outcomes of both approaches are analyzed by three RBD considerations: (I) subjective back-calculated mean values of soil parameters; (II) minimum and maximum values of soil variability reported in the literature; and (III) verification of strength and stability of the embedded wall by rotational failure, hydraulic failure, and system failure. The reliability levels of the design outcomes of the codes are compared by generalized subset simulations (GSS).

2 Methodology

2.1 Limit-state design approaches

Tables 1 and 2 show the limit-state design approaches of the AASHTO LRFD BDS and EN 1997-1:2004 codes for embedded wall design. In the USA, the limit-state design approach (or, load and resistance factor design-LRFD) is based on a factored resistance approach. The limit-state design equation can be expressed as

$$\sum \gamma_i Q_{ni} \leq \varphi R_n \tag{1}$$

where Q_{ni} is the nominal load; R_n is the nominal resistance; γ_i is the load factor; φ is the resistance factor. The load factor terms have values $\gamma_i \geq 1$, while the resistance term should have a value $\varphi \leq 1$ (see Table 1).

In Europe, the limit-state design approach of the EN 1997-1:2004 code that involves the verification of the strength of the ground (i.e., limit-state GEO) is based on two factored strength approaches (DA1 and DA3) and a factored resistance approach (DA2) (see Table 2). The limit-state design equation can be expressed as

$$E_d \leq R_d \tag{2}$$

where E_d is the design effect of actions and R_d is the corresponding resistance to that effect. Safety is incorporated into the limit-state design by the introduction of partial factors, as shown in Eq. (3).

Table 1. Limit-state design approaches of the AASHTO and EN 1997-1:2004 codes for the design of embedded walls.

Design code	Country/ Community	Theory		Load and resistance factors	Wall friction Sand/Steel
		Active (K_a)	Passive (K_p)		
EN 1997-1:2004 Limit-states GEO and HYD	Europe Union	Analytical EN 1997-1:2004 Annex C	Analytical EN 1997-1:2004 Annex C	Partial factors (see Table 2)	$\delta'_d=2/3\phi'_d$ $\tan\phi'_d=(\tan\phi'_k)/\gamma_{\phi'}$
AASHTO LRFD BDS (2020) Load Combination: Strength I	USA	Coulomb	Caquot and Kerisel	γ_{EH}=1.5 γ_{ES}=1.5 γ_{WA}=1.0 φ=0.75	$\delta'=2/3\phi'_k$

Table 2. Partial factors for the design of embedded walls.

Partial factor for	DA1		DA2	DA3
	C1	C2	-	-
Unfavorable permanent actions, $\gamma_{G,unfav}$	1.35	1.0	1.35	1.0
Unfavorable variable actions, $\gamma_{Q,unfav}$	1.5	1.3	1.5	1.3
Effective friction angle, $\gamma_{\phi'}$	1.0	1.25	1.0	1.25
Earth resistance, γ_R	1.0	1.0	1.4	1.0

$$\gamma_E E\left\{F_d=\gamma_F\psi_i F_k, X_d=\frac{X_k}{\gamma_M}, a_d=a_{nom}\pm\Delta a\right\}\le\frac{R\left\{F_d=\gamma_F\psi_i F_k, X_d=\frac{X_k}{\gamma_M}, a_d=a_{nom}\pm\Delta a\right\}}{\gamma_R} \quad (3)$$

in which F_d, X_d, and a_d are design values of actions, material properties, and geometry, respectively; γ_E and γ_R are partial factors on the effects of actions and resistance; F_k, ψ_i, X_k, and a_{nom} are characteristic values of actions, combination factors of actions, characteristic material properties, and nominal dimensions, respectively; γ_F and γ_M are partial factors on the actions and material properties; Δa is a tolerance or safety margin on the geometry.
The limit-state design approach of the EN 1997-1:2004 code that involves the verification of stability against hydraulic heave (i.e., limit-state HYD) is expressed by Eqs. (4) and (5).

$$u_{d,dst}\le\sigma_{d,stb} \quad (4)$$

$$S_{d,dst}\le G'_{d,stb} \quad (5)$$

in which $u_{d,dst}$ is the design value of the destabilizing water pressure; $\sigma_{d,stb}$ is the design value of the stabilizing total stress in the ground; $S_{d,dst}$ is the design value of the destabilizing seepage force in the ground; $G'_{d,stb}$ is the design value of the stabilizing permanent vertical effective actions for heave verification.Eqs. (4) and (5) are known as the total stress method and the seepage force method, respectively(Bond and Harris 2008). Details of the partial factors of the limit-state HYD are not provided herein for the sake of conciseness.

2.1.1 Characteristic values

Clause 4.1.2(7)P of the EN 1990:2002 code state that for variable actions, the characteristic value shall correspond to one of the following: *an upper value with an intended probability of not being exceeded or a lower value with an intended probability of being achieved (...)*; or *a nominal value, which may be specified in cases where a statistical distribution is not known.*Fenton et al. (2016) describe this definition as *fairly vague*.Besides, they interpret Clause 4.1.2(4) as meaning that an *upper value* (which would be of interest for loads) corresponds to a 5% probability of being exceeded (95% fractile), and also that the variable actions may be assumed to be Gaussian.

Based on the above, in this study, it is considered that the characteristic value for a variable action (Q_k)is the action magnitude that corresponds to a 5% probability of being exceeded, i.e., an upper 95% fractile. If the action follows a lognormal distribution, then the upper 95% fractile is given by Eq. (6).

$$ln(Q_k)=\mu_{ln\,Q}+1.645\sigma_{ln\,Q} \quad (6)$$

where the mean and standard deviation of ln(Q_k) are determined as $\mu_{\ln Q}=\ln(\mu_Q)-0.5\sigma^2_{\ln Q}$and $\sigma^2_{\ln Q}=\ln(1+COV_Q^2)$; μ_Q and COV_Q are the mean and coefficient of variation of the variable action, respectively.

Hicks (2013) and Schneider and Schneider (2013) interpret Clause 2.4.5.2(11) of the EN 1997-1:2004 codeas meaning that if statistical methods are used, the characteristic value of a geotechnical parameter (X_k)may be selected as the lower 5% fractile of the parameter values.Thus, if the geotechnical parameter follows a lognormal distribution, then the lower 5% fractile is given by Eq. (7).

$$\ln(X_k)=\mu_{ln\,x}-1.645\sigma_{ln\,x} \quad (7)$$

where the mean and standard deviation of ln(X_k) are determined as $\mu_{\ln x}=\ln(\mu_x)-0.5\sigma^2_{\ln x}$and $\sigma^2_{\ln x}=\ln(1+COV_x^2)$; $\mu_x$and COV_x are the mean and coefficient of variation of the geotechnical parameter, respectively.

2.2 MCS-based probabilistic design approach

For embedded walls, the MCS-based probabilistic design approach is based on generating a frequency histogram of an output random variable (e.g., embedment depth) from random samples of one or more input variables. In a spreadsheet-based environment, the generation of random samples of the input random variables is performed by the inverse transformation method. The input and output random variables are linked by a design equation [e.g., Eq. (1)]. This probabilistic approach allows failure percentiles to be determined by Eq. (8).

$$P_f = P\left[d_{min} > d\right] = 1 - P\left[d_{min} \le d\right] \tag{8}$$

In Eq. (8), failure of an embedded wall occurs when the final design embedment depth (d) is less than the minimum design embedment depth (d_{min}). The minimum design parameter (d_{min}) corresponds to the minimum value of the frequency histogram.The probability of failure (P_f) from Eq. (8) is equivalent to the complement of the cumulative probability distribution generated from the histogram of the embedment depth(Wang 2013; Mattos et al. 2021). The expected performance level of a structure is also expressed in terms of the reliability index which is calculated as $\beta=-\Phi^{-1}(P_f)$, where $\Phi^{-1}(.)$ is the inverse of the standard normal cumulative function.

2.3 Generalized subset simulations

The GSS computation process consists of generating unconditional samples from a direct MCS. Values of $Y^{(j)}$ are then computed for each possible design $D^{(j)}$ and ranked in ascending order to define $y_m^{(j)}$ such that the sample estimate for $P(F_1^{(j)})=P(Y^{(j)}>y_1^{(j)})$ is equal to p_0. This procedure is repeated for each possible design based on the N samples to determine their respective $y_1^{(j)}$, j=1, 2, …, N_D, based on which a number of p_0N samples with $F_1^{(j)}=\{Y^{(j)}>y_1^{(j)}\}$areselected for each possible design. After that, $F_{U,1}$is determined as $F_U=F_1^{(1)}\cup\ldots\cup F_1^{(j)}\cup\ldots\cup F_1^{(ND)}$, j=1, 2, …, N_D. The probability $P(F_{U,1})$ is estimated as N_1/N. The N_1 samples in $F_{U,1}$are used as seed samples to simulate N-N_1 conditional samples in $F_{U,1}$ (see Appendix).The above procedure is repeatedly performed$M$ times to simultaneously approach failure domains of the N_D possible designs until $P_f^{(j)}<P_T$ is achieved. A total of M+1 levels of simulation chains are performed, providing $N+\sum_{m=1}^{M}(N-N_m)$samples.Let $M^{(j)}$ denote the number of simulation levels needed to reach the failure domain $F^{(j)}$ of $D^{(j)}$. Using the samples generated by the GSS, the $P_f^{(j)}$ is estimated as

$$P_f^{(j)} = P\left(F^{(j)}\right) = P\left(F_{U,1}\right)P\left(F_{U,2}|F_{U,1}\right)\ldots P\left(F_{U,M^{(j)}-1}|F_{U,M^{(j)}-2}\right)P\left(F^{(j)}|F_{U,M^{(j)}-1}\right) = \prod_{m=1}^{M^{(j)}-1}\frac{N_m}{N}\times\frac{N^{(j)}}{N} \tag{9}$$

in which $P(F_{U,1})=N_1/N$; $P(F_{U,m}|F_{U,m-1})$, m=2, 3, …, $M^{(j)}$-1, is calculated as the ratio of the number of seed samples $N_m$selected for the m-th level among conditional samples in $F_{U,m-1}$over N; $P(F^{(j)}|F_{U,M^{(j)}-1})$ is determined as the ratio of the number $N^{(j)}$ of failure samples belonging to $F^{(j)}$ among conditional samples generated in $F_{U,M^{(j)}-1}$over N(Cao et al. 2019; Gao et al. 2019).

2.4 Reliability modeling considering a case study

Figure 1 shows a cantilever sheet pile wall embedded in cohesionless soil. Behind the wall, the water table (WT) is at the same depth as the dredge level. In front of the wall, the WT is d_w=1 m below the dredge level. A surcharge q_k=10 kPa acts on the retained soil surface. The embedment depth of the wall (d) is determined by rotational failure and hydraulic failure to the codes and reliability approaches. This problem was proposed by Knappett & Craig (2019) with a balance of the water pressures». The characteristic values of the soil parameters are shown in Figure 1. Regarding diagrams (1)-(9) they correspond to surcharge pressure (1); total earth pressures (2), (3), (7), and (8); effective earth pressures (4) and (9); and water pressures (5) and (6). The surcharge pressure and total earth pressures are calculated with the theories and wall friction shown in Table 1.

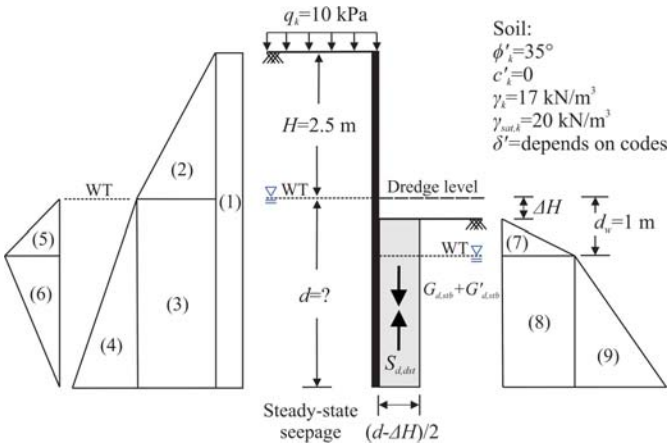

Figure 1. Embedded sheet pile wall.

In the MCS-based probabilistic design approach, the effective friction angle (ϕ'),soil unit weight(γ), saturated soil unit weight (γ_{sat}), and surcharge (q) are modeled as lognormal random variables. Rotational and hydraulic failures are modeled by using the mean values instead of the characteristic values of the surcharge and soil parameters. The mean values are back-calculated by Eqs. (6) and (7) considering the coefficient of variations shown in Table 3.Besides, the partial factors, load and resistance factors, and over dig allowance are omitted from the reliability modeling. Wall friction is modeled as $\frac{2}{3}\phi'$.The MCS-based probabilistic modeling is performed in a spreadsheet-based environment using @Risk(Palisade Corporation, 2022). In this study, the simulations are performed with 1,200,000 random samples; they exceeded the minimum number of random samples (1,110,000) required to reach a target probability of failure of 0.1% and a coefficient of variation of the target probability of 3%(Mattos 2022).

Table3. Variability of the soil parameters and surcharge.

$COV_{\varphi'}$	COV_{γ}	$COV_{\gamma sat}$	COV_q
Min=5% Max=15%	5%	5%	15%

In the GSS, the random variables are the same as those considered in the MCS-based probabilistic design approach. The design parameter is the embedment depth (i.e., $D^{(j)}=d$), which is considered to vary from 2 to 8 m at an interval of 0.2 m, resulting in a total of N_D=31 possible designs.Three driving variables are considered, corresponding to rotational and hydraulic failure separately and to system failure, i.e., $1/FS_R$, $1/FS_H$, max{$1/FS_R$, $1/FS_H$}. The GSS-based full probabilistic modeling is performed in a spreadsheet-based environment using GeoRBD/S (Cao et al. 2019). The GSS are performed considering N=10,000 random samples for the direct MCS from which$M$=4 levels of subsets simulations are generated to achieve $P_f^{(j)}<3.17\times10^{-5}$ (i.e.,$\beta^{(j)}>4$) withp_0=0.1. This model configuration achieves high-resolution results at small probability levels$P_f^{(j)}>5.99\times10^{-9}$for most designs in the selected domain of d, as shown in the results.

3 Results and discussions

Figure 2a shows the MCS-based probabilistic designs for rotational failure expressed in terms of the reliability index. Two subjective back-calculated mean values of the unit weight (γ) and saturated unit weight (γ_{sat}) are considered. In each design, the mean value of ln(q) is calculated by Eq. (7) withCOV_q =15%. The mean value of ln(φ') is calculated by Eq. (6) considering the max. or min. variability of ϕ'as appropriate (see Table 3).The mean values of ln(γ) and ln(γ_{sat}) are both determined by Eq. (6) if they are considered as the 5%fractile of their lognormal distributions. In all designs $COV_{\gamma}=COV_{\gamma sat}$=5%. The legend of Figure 2a has the following meaning:

- *p5-Min* is based on the 5% fractile (percentile) for both γ and γ_{sat}, and COV_{φ}=5%
- *p95-Min* is based on the 95% fractile for both γ and γ_{sat}, and COV_{φ}=5%
- *p5-Max*is based on the 5% fractilefor both γ and γ_{sat}, and COV_{φ}=15%
- *p95-Max*is based on the 95% fractile for both γ and γ_{sat},andCOV_{φ}=15%

The reason for considering subjective back-calculated mean values derives from the possibility that a practitioner may note that the soil unit weights γ and γ_{sat} contribute to the active pressure and it regards them as unfavorable load parameters. Thus, the practitioner may perform a subjective design with the upper 95% fractile for γ and γ_{sat}, contrary to the guidelines of Clause 2.4.5.2(11) of the EN 1997-1:2004 code.

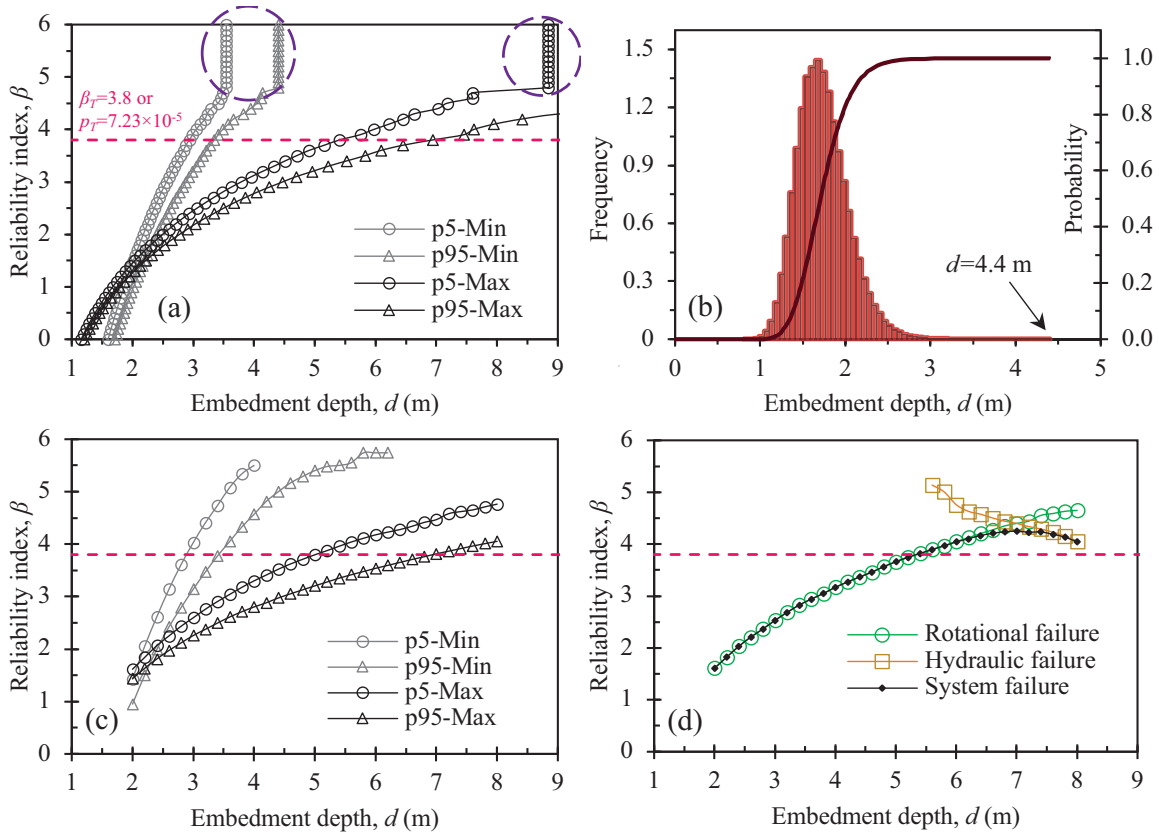

Figure 2. Direct probability-based embedment depth:(a) MCS of rotational failure; (b) output histogram of MCS*p95-Min*; (c) GSS of rotational failure; (d) GSS of system failure.

Figure 2a shows a dual sensitivity analysis for subjective back-calculated mean values of γ and γ_{sat} and variability of ϕ'. The effect of the variability of ϕ' (aleatory uncertainty) on the wall design is greater than that produced by the back-calculated mean values (epistemic uncertainty) at small probability levels. The effect of both uncertainties is reflected, for instance, at β_T=3.8 where the most critical design is *p5-Min* (d=2.93 m) and the most conservative is *p95-Max* (d=6.94 m). The dashed circles show that the MCS-based probabilistic design approach leads to errors at reliability indexes $\beta > 4.8$. This is because the failure percentiles reach a maximum value of the embedment depth in the cumulative probability distribution. In the case of *p95-Min*, the maximum value is d=4.4 m, as shown by the histogram in Figure 2b.

Tables 3 and 4 show that a large coefficient of variation of an input parameter propagates to a large coefficient of variation of the response, i.e., d because the response is sensitive to the input parameter. The greatest uncertainty propagation is evidenced in the *p95-Max* design in which the coefficient of variation of the embedment depth COV_d=76.2% is 61.2% (76.2%-15%=61.2%) greater than the coefficient of variation of the effective friction angle. «It should be noted that the statistical properties of Table 4 do not include the error values, otherwise, the propagation of the uncertainty would be 62.8% greater than COV_φ=15%». The above analyzes demonstrate that the MCS-based probabilistic design approach is highly susceptible to the effect of the aleatory and epistemic uncertainties and uncertainty propagation.

Figure 2c shows the GSS-based full probabilistic designs for rotational failure. The GSS shows high-resolution results at small probability levels compared to the MCS-based probabilistic design approach. For the selected domain of d, the reliability indexes range from β=1 to β=5.7. In the GSS, the probability of failure $P_f^{(j)}$ does not depend on an output histogram, which avoids errors at small probability levels, such as those observed in Figure 2a. The influence of the aleatory and epistemic uncertainties also have a significant effect on GSS. At β_T=3.8, the most critical design is *p5-Min* (d=2.89 m), and the most conservative is*p95-Max* (d=6.95 m). Both reliability approaches (MCS and GSS) achieve similar results, but GSS requires fewer random samples. Among the four GSS-based full probabilistic designs, the one that demands the most significant computational effort (i.e., *p95-Min*) required 54,049 random samples to achieve $\beta^{(j)} > 4$.

Table 4. Statistical properties of the *d* output histograms.

Embedded depth, *d* (m)				
MCS	*p5-Min*	*p95-Min*	*p5-Max*	*p95-Max*
Mean	2.41	2.71	3.55	4.59
St. Dev.	0.57	0.74	2.09	3.50
COV_d	23.8%	27.4%	58.7%	76.2%

Figure 2d shows the GSS-based full probabilistic design for the system failure. The embedment depth exhibits a dual behavior; it is stabilizing for rotational failure and destabilizing for hydraulic failure. The duality of *d* is because it has a destabilizing effect on the system by S_{dst} and u_{dst} via average hydraulic gradient i_{avg}=½(2*d*-d_w)/(*d*-d_w), and a stabilizing effect by passive pressures via γ and γ'_{sat}-$i\gamma_w$ with i=d_w/(2*d*-d_w). The i_{avg} arises from the average hydraulic head acting over the base of the shaded soil columns hown in Figure 1. The $i_{avg}$is used in well-known European textbooks (e.g., Bond & Harris, 2008; HTG, 2015). In this study, the difference between using *i*and i_{avg} for hydraulic heave is that the former does not lead to failure and the latter does. The duality of *d* has an important repercussion in the system design because the results may lead to two depths with the same reliability (see Figure 2d), which adds uncertainty to the direct probability-based design.

One of the disadvantages of the GSS is that the domain of $D^{(j)}$ and the number of possible designs, N_D, must be calibrated to reach the reliability levels of interest for the failure modes to be considered. It may occur that in some cases the selected domain leads to failure for one mode and not for another, or that for a failure mode the selected domain has $P_f^{(j)}$ values so close to zero that the GSS cannot compute them. In this study, the second case occurred, for the selected domain, $P_f^{(j)}$=0 values were obtained for d < 5.6 m for the hydraulic failure. One limitation of the GSS may be that for a practitioner trained to apply reliability in the simple format of codes (e.g., LRFD), the GSS would be difficult to apply because it is conceptually more complex. This limitation has important consequences in the design practice because it can lead to the reliability approach being used incorrectly (i.e., uncertainty in the knowledge development and utilization).

Table 5 shows the reliability levels of the limit-state design approaches of the codes for the embedded wall design. The reliability index values are evaluated based on Figure 2d, which shows the rotational failure and hydraulic failures considering the highest variability of the effective friction angle reported in the literature (see Table 3). The embedment depth (*d*) calculated by DA1.C1 is less than that calculated by DA1.C2; therefore, DA1.C2 is chosen to represent DA1 as it requires a greater embedment depth than DA1.C1 to prevent failure. This result is consistent with the Farrell & Orr (1998)analyses, which show that DA1.C1 does not provide a sufficient margin of safety against rotational failure because the values of the partial factor $\gamma_{G,unfav}$=1.35applied to the water pressures and earth pressures cancel each other out when evaluating the equilibrium by Eq. (2).

Table 5 also shows that there is a wide difference between the reliability levels of the DA2 and Strength I approaches. This difference derives from the fact that DA2 increases water pressures by a factor of $\gamma_{G,unfav}$=1.35while Strength I increases them by γ_{WA}=1.0. In addition, the design approaches of the EN 1997-1:2004 code consider an overdig allowance, while the AASHTO LRFD BDS code does not. The reliability levels (β) of the limit-state design approaches exceed the prescribed target reliability indexes, which are β_T=3.8 and β_T=2.0 for the EN 1997-1:2004 and AASHTO LRFD BDS codes, respectively.

4 Conclusions

The load-resistance duality of the AASHTO LRFD BDS and EN 1997-1:2004 codes was analyzed. The DA1.C1 approach of the EN 1997-1:2004 code, which considers the active and passive pressures of the wall as loads, was determined to lead to the most critical design. In contrast, the most conservative result was obtained for DA1.C2 which increases the active pressures by a factor of $\gamma_{G,unfav}$=1.35, reduces the favorable effect of the soil friction (tan ϕ') to 80% (i.e., 1/1.25), and keeps the passive pressures unfactored.

Table5. Reliability indexes achieved by the limit-state approaches of the codes.

Limit-state	Approach	*d* (m)	P_f	β	(β-β_T)/β_T [%]
GEO	DA1.C1	3.19	3.64×10^{-3}	2.68	-29.5%
	DA1.C2 (=DA3)	6.21	1.86×10^{-5}	4.12	8.4%
	DA2	5.63	4.67×10^{-5}	3.91	2.9%
Rotational	AASHTO Strength I	4.04	7.15×10^{-4}	3.19	59.4%
HYD	Hydraulic failure	2.19	0	-	-

The limit-state design approaches of the codes were found to lead to the overdesign of an embedded sheet pile wall compared to direct probability-based design approaches. This result answers the question asked at the

XVI Danube European Conference: Are we overdesigning? (Ching and Zhang 2020). Although the case study shown herein is overdesigned by the principles of the codes, the analysis should be extended to other case studies and reliability-based design methods.

A limitation of advanced Monte Carlo methods in geotechnics is that the calculatedP_f dependson the random distribution of the soil parameters and actions/loads.This does not allow general conclusions to be drawn about the exact safety level or β_T value corresponding to a limit-state design because these values change if different assumptions are made concerning random variables. It is more efficient and realistic to analyze the possible ranges of these values and investigate the design's sensitivity to changes in the assumptions regarding the geotechnical parameters.

Acknowledgments

The authors wish to give special thanks to Dr.Zijun Cao from Wuhan University for providing the GeoRBD/S software. This work was supported by the Student–Instructor Fellowship (Dean's Resolution No. 0057 of 2021) of the Faculty of Engineering, University of Antioquia. The financial support is gratefully acknowledged.

Appendix: GSS definitions

$D^{(j)}$: possible designs; N_D: number of possible designs; N_F: number of failure modes of $D^{(j)}$
$Y^{(j)}$: driving variable of the system, i.e., $\max\{1/FS_1^{(j)}, 1/FS_k^{(j)}, \ldots, 1/FS_{NF}^{(j)}\}$
$1/FS_k^{(j)}$: reciprocal of the factor of safety values of the N_F failure modes of $D^{(j)}$
F_U: union of system failure events of the N_D possible designs, i.e., $F_U=F^{(1)}\cup \ldots \cup F^{(j)}\cup \ldots \cup F^{(ND)}$
$F_{U,I}$: union of intermediate events (i.e., $F_1^{(j)}$, j=1, 2, …, N_D) of the N_D design in the m-th simulation level
$y_m^{(j)}$: intermediate threshold value of $D^{(j)}$ in the m-th simulation level
p_0: conditional probability, i.e., number of samples such that $P(F_m^{(j)})=P(Y^{(j)}>y_m^{(j)})$

References

AASHTO (2020). AASHTO LRFD Bridge Design Specifications (9th ed.). *Washington D.C.: AASHTO*.

Bond, A., & Harris, A. (2008).Decoding Eurocode 7. *London: Taylor & Francis*.

Cao, Z.-J., Gao, G.-H., Li, D.-Q., & Wang, Y. (2019). Values of Monte Carlo Samples for Geotechnical Reliability-Based Design. *7th ISGSR. Singapore: Research Publishing.*

CEN (2002). *Eurocode - Basis of Structural Design. EN 1990:2002*. Brussels: CEN.

CEN (2004). *Eurocode 7: Geotechnical design - Part 1: General rules. EN 1997-1:2004*. Brussels: CEN.

Ching, Jianye, & Zhang, J. (Eds.). (2020). Probabilistic solutions for survey questions in "Are we overdesigning?-A survey of international practice.*ISSMGE TC304*.

Christian, J. T., & Baecher, G. B. (2011). Unresolved Problems in Geotechnical Risk and Reliability. *GeoRisk 2011. ASCE*.

Farrell, E. R., & Orr, T. L. L. (1998). Safety of retaining walls with high water loadings when designed to Eurocode 7 using partial factors. *Ground Engineering*, 31(10), 37–40.

Fenton, G. A., Naghibi, F., Dundas, D., Bathurst, R. J., & Griffiths, D. V. (2016). Reliability-based geotechnical design in 2014 Canadian Highway Bridge Design Code. *Can. Geotech. J*,53(2), 236–251.

Gao, G.-H., Li, D.-Q., Cao, Z.-J., Wang, Y., & Zhang, L. (2019). Full probabilistic design of earth retaining structures using generalized subset simulation. *Computers and Geotechnics*, 112(8), 159–172.

Hicks, M. A. (2013). An Explanation of Characteristic Values of Soil Properties in Eurocode 7. *Modern Geotechnical Design Codes of Practice*. *Amsterdam: IOS Pres*s.

HTG (2015). Recommendations of the Committee for Waterfront Structures Harbours and Waterways EAU 2012 (9th ed.). *Hamburg: Wilhelm Ernst & Sohn*.

ISO (2015). ISO 2394:2015 General principles on reliability for structures (ISO/TC98/SC2) (4th ed.). *Geneva: ISO*.

Knappett, J., & Craig, R. F. (2019). Craig's Soil Mechanics (9th ed.). *London: CRC Press*.

Low, B. K., & Bathurst, R. J. (2021). Load-resistance duality and case-specific sensitivity in reliability-based design. *Acta Geotechnica*, 4.

Mattos, Á. J. (2022). Reliability Analysis of Modern Geotechnical Codes for the Limit State Design of Sheet Pile Structures Considering Parameter Uncertainties. *Int. J. Geomech*, 22(3).

Mattos, Á. J., Viviescas, J. C., & Osorio, J. P. (2021). Reliability Comparative Analysis of Codes for the Design of Cantilever Sheet Pile Walls: Basis for Studying the Principles of International Standards. *Int. J. Geomech*, 21(5).

Palisade Corporation. (2022). @Risk v8.2.2 Industrial Edition. *Palisade*.

Schneider, H. R., & Schneider, M. A. (2013). Dealing with uncertainty in EC7 with emphasis on the determination of characteristic soil properties. *Modern Geotechnical Design Codes of Practice. Amsterdam: IOS Press*.

Wang, Y. (2013). MCS-based probabilistic design of embedded sheet pile walls. *Georisk7*(3), 151–162.

Wang, Y., Schweckendiek, T., Gong, W., Zhao, T., & Phoon, K.-K. (2016). Direct probability-based design methods. *Reliability of Geotechnical Structures in ISO2394. London: CRC Press/Balkema*.